

# Image Cover Sheet

**CLASSIFICATION**

UNCLASSIFIED

**SYSTEM NUMBER**

507460



**TITLE**

NON-LOCAL BOUNDARY CONDITONS FOR 1-WAY WAVE PROPAGATION

**System Number:**

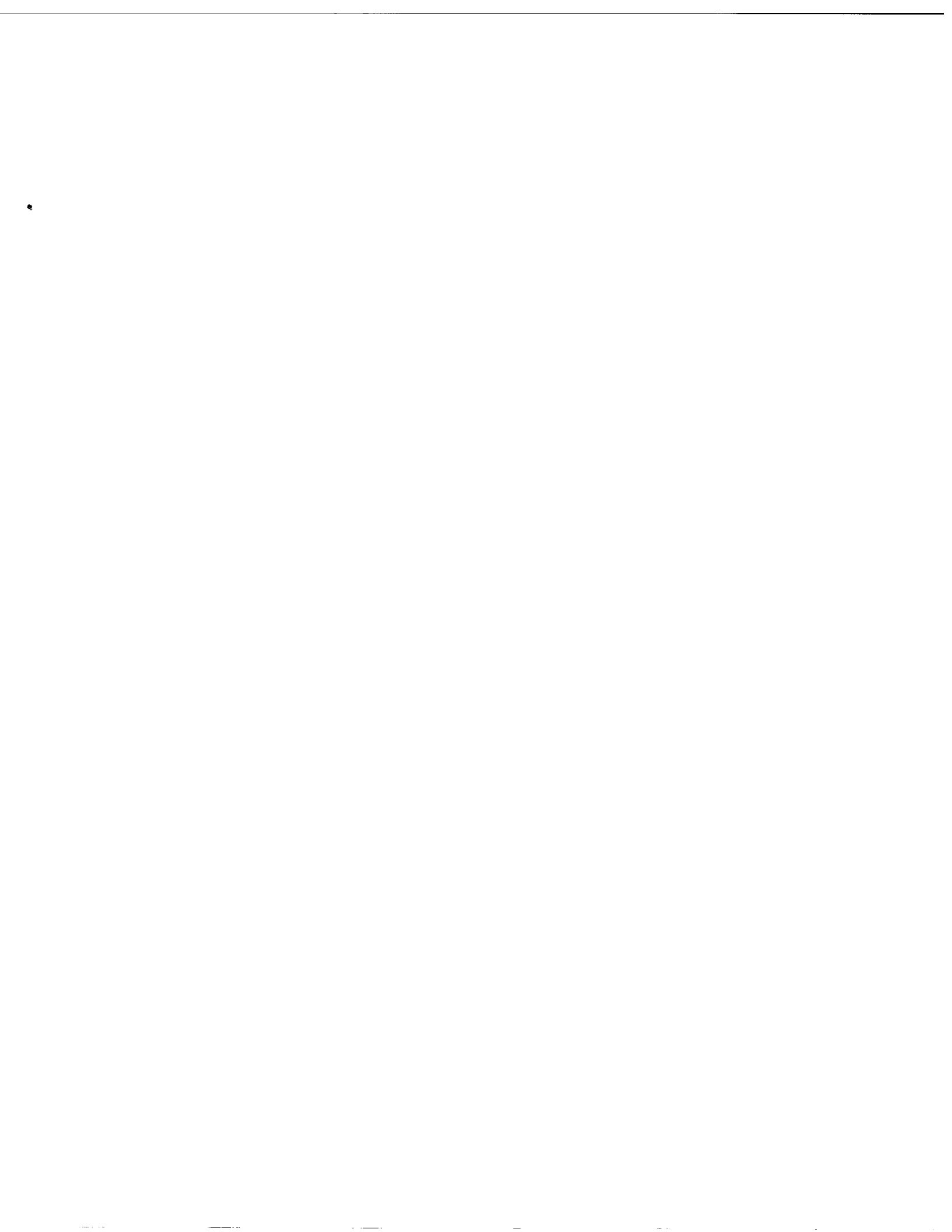
**Patron Number:**

**Requester:**

**Notes:**

**DSIS Use only:**

**Deliver to:**



# Non-local Boundary Conditions for 1-Way Wave Propagation

David J. Thomson\*

Gary H. Brooke†

## Abstract

In sonar (radar) parabolic equation (PE) solvers, the downgoing (upgoing) radiation condition is usually approximated by appending an absorbing layer to the computational mesh. Alternatively, non-local boundary conditions (NLBCs) can be used that exactly transform the semi-infinite PE problem with a radiation condition at infinity into an equivalent PE problem in a bounded domain. Here we review two schemes for deriving and incorporating NLBCs into PE codes that are solved by finite-difference methods.

## 1 Introduction

Many sonar and radar applications involve waveguide propagation cast in terms of one-way waves that satisfy a parabolic equation (PE). This is convenient, since a PE is amenable to efficient numerical solution by marching algorithms (see [1, pp. 343–412] and the references therein). If a physical boundary of the waveguide is penetrable (e.g., the sea bottom), then a transverse radiation condition must be imposed on those field components that propagate across the boundary to infinity. This condition is usually approximated by appending an *ad hoc* absorbing layer to the computational mesh. In this paper, we review the concept of using a non-local boundary condition (NLBC) to *exactly* convert the PE problem with a transverse radiation condition at infinity into an equivalent PE problem in a bounded domain [2]–[4].

## 2 Parabolic Equations

We focus on the sonar problem. The set up for the radar problem is similar. Let the half-space  $z > 0$  in  $(r, z)$ -space contain a fluid with density  $\rho$  and sound speed  $c$ . It is convenient to set  $N = n(1 + i\alpha)$  where  $\alpha$  accounts for absorbing media. Here,  $n = c_0/c$  is the acoustic refractive index and  $k_0 = \omega/c_0$  is a reference wavenumber. Within  $0 < z < z_b$ , both  $\rho$  and  $N$  can vary with range  $r$  and depth  $z$ . For  $z > z_b$ , however, these material properties are assumed to be functions of depth only. Subscripts “ $\pm$ ” will be used to denote quantities evaluated at  $z_b \pm 0$ . The goal is to obtain an NLBC along the plane  $z = z_b$  in order to confine the computational domain over which the PE+NLBC problem is numerically solved.

For  $r > 0$ , the outgoing component of the pressure,  $p(r, z) = \psi(r, z) \exp(ik_0 r) / \sqrt{r}$ , due to a harmonic  $\exp(-i\omega t)$  point source at  $(r, z) = (0, z_s)$ , can be obtained from the step-by-step numerical solution of the evolution equation [5]

$$(1) \quad \frac{\partial \psi}{\partial r} = ik_0 \left\{ -1 + \sqrt{1 + X} \right\} \psi \approx ik_0 \sum_{j=1}^J \frac{a_j X}{1 + b_j X} \psi,$$

---

\*Defence Research Establishment Atlantic, P.O. 1012, Dartmouth, N.S. B2Y 3Z7

†Integrated Performance Decisions, Suite 8A, 947 Fort Street, Victoria, B.C. V8V 3K3

where  $a_j$  and  $b_j$  are coefficients of the Padé approximation to the square-root operator and  $X$  denotes  $N^2 - 1 + k_0^{-2} \rho \partial_z (\rho^{-1} \partial_z)$ . Because range-dependent media are usually modeled as a sequence of range-independent segments, (1) can be solved between  $r$  and  $r + \Delta r$  as a sequence of  $J$  systems of equations. The  $j$ th system is given by

$$(2) \quad (1 + b_j X) \frac{\partial \psi_j}{\partial r} = ik_0 a_j X \psi_j.$$

The Crank-Nicolson algorithm for solving (2) combines the approximations

$$(3) \quad \begin{aligned} \frac{\partial \psi_j}{\partial r} &\approx \frac{\psi(r_j, z) - \psi(r_{j-1}, z)}{\Delta r}, \\ \psi_j &\approx \frac{\psi(r_j, z) + \psi(r_{j-1}, z)}{2}, \end{aligned}$$

with a finite-difference representation for  $X\psi$  to yield  $J$  implicit tri-diagonal systems of equations where  $r_j = r + \frac{j\Delta r}{J}$  for  $j = 1, \dots, J$ . Here, we consider only single-term approximations to  $\sqrt{1 + X}$ . When  $J = 1$ ,  $a_1 = \frac{1}{2}$  and  $b_1 = \frac{1}{4}$  and (2) leads to a third-order, rational-linear PE. The standard second-order PE is obtained by setting  $b_1 = 0$ .

### 3 Non-local Boundary Conditions

We describe two methods for deriving non-local boundary conditions along  $z = z_b$ . The first method requires that the region  $z > z_b$  be a uniform fluid.

#### 3.1 Method I

The standard PE in  $z > z_b$  is given by

$$(4) \quad 2ik_0 \frac{\partial \psi}{\partial r} + \frac{\partial^2 \psi}{\partial z^2} + k_0^2 (N_+^2 - 1) \psi = 0.$$

Using the approximations in (3), (4) can be put in the form

$$(5) \quad (\delta + X_+) \psi(r + \Delta r, z) = (\delta - X_+) \psi(r, z),$$

where  $\delta = 4i / (k_0 \Delta r)$ . Introducing the range-translation operator  $\mathcal{T} = \exp(-\Delta r \partial_r)$  and noting that  $\mathcal{T}^j \psi(r, z) = \psi(r - j\Delta r, z)$ , (5) can be re-arranged as

$$(6) \quad \left\{ \frac{\partial^2}{\partial z^2} + \mathcal{G}_0^2 \right\} \psi(r + \Delta r, z) = 0,$$

where  $\mathcal{G}_0$  is the vertical-wavenumber operator defined by

$$(7) \quad \mathcal{G}_0^2 = k_0^2 \left( N_+^2 - 1 + \delta \frac{1 - \mathcal{T}}{1 + \mathcal{T}} \right).$$

For the downgoing factor of (6), continuity of impedance  $i\omega \rho \psi / \psi_z$  across  $z = z_b$  yields the non-local boundary condition

$$(8) \quad \left\{ \frac{\partial}{\partial z} - i(\rho_- / \rho_+) \mathcal{G}_0 \right\} \psi(r + \Delta r, z_b) = 0.$$

A tractable form of (8) suitable for numerical implementation results by expanding  $\mathcal{G}_0$  in a power series in  $\mathcal{T}$ . The same procedure can be applied to the rational-linear PE and leads to an NLBC similar to (8) but with a different expression for the vertical wavenumber operator [6].

### 3.2 Method II

The standard PE within a thin homogeneous layer  $z_b - \delta < z < z_b$  is given by

$$(9) \quad 2ik_0 \frac{\partial \psi}{\partial r} + \frac{\partial^2 \psi}{\partial z^2} + k_0^2 (N_-^2 - 1) \psi = 0.$$

The half-range Fourier transform of (9) in this region can be written as

$$(10) \quad F(s, z) \equiv \int_0^\infty \psi(t, z) e^{-ist} dt = A(s) \left\{ e^{i\gamma_-(s)|z-z_b|} + R(s) e^{-i\gamma_-(s)|z-z_b|} \right\},$$

where  $R(s)$  is the plane-wave reflection response of the medium in  $z > z_b$ ,

$$(11) \quad \gamma_-(s) = k_0 \sqrt{N_-^2 - 1 - 2s/k_0} \equiv \sqrt{k_0^2 N_-^2 - k^2}$$

is the vertical wavenumber of a plane wave incident from  $z < z_b$ , and  $k$  is its horizontal component [7]. Forming the ratio  $F/F_z$  at  $z = z_b$  using (10) yields the local impedance-type condition

$$(12) \quad G(s) \equiv \frac{F}{\partial F / \partial z} \Big|_{z=z_b-0} = \frac{1}{i\gamma_-(s)} \frac{1 + R(s)}{1 - R(s)}.$$

Applying the inverse transform to (12) leads to the non-local boundary condition [8, 9]

$$(13) \quad \psi(r, z_b) = \frac{1}{2\pi} \int_0^r \psi_z(t, z_b) \underbrace{\left( \int_{-\infty}^\infty G(s) \exp[is(r-t)] ds \right)}_{g(r-t)} dt.$$

This form of the NLBC accounts for any medium in  $z > z_b$  for which  $R(s)$  can be specified.

### 3.3 Reflection Coefficients

The reflection coefficient for a uniform solid half-space is known to be [10]

$$(14) \quad R_f(s) = \frac{\gamma_-(s) - (\rho_-/\rho_+) \gamma_+(s)/P(s)}{\gamma_-(s) + (\rho_-/\rho_+) \gamma_+(s)/P(s)},$$

where  $P(s) = (1 - 2k^2(s)/N_s^2)^2 + 4k^2(s)\gamma_s(s)\gamma_+(s)/N_s^4$  contains the shear properties of the bottom. Substituting (14) into (12) gives

$$(15) \quad G_s(s) = \frac{(\rho_-/\rho_+) P(s)}{i\gamma_+(s)}.$$

In previous work [8, 9],  $g$  was determined numerically before discretizing the NLBC in (13). Recently, the inverse transform of (15) has been obtained analytically [11].

Noting that  $P \rightarrow 1$  as  $N_s \rightarrow \infty$ ,  $g$  for a fluid half-space can be found analytically and (13) evaluates to [4, 7, 8]

$$(16) \quad \psi(r, z_b) = B \int_0^r \psi_z(t, z_b) \frac{\exp[ib(r-t)]}{\sqrt{r-t}} dt,$$

where  $B = -(\rho_-/\rho_+) \sqrt{i/\sqrt{2\pi k_0}}$  and  $b = \frac{1}{2}k_0 (N_+^2 - 1)$ . This expression is an alternative to the one given in (8). We note that an absorbing (transparent) boundary along  $z = z_b$  is

obtained by setting  $R(s) = 0$  in (7), or, equivalently, letting  $\rho_- = \rho_+$  and  $N_- = N_+$  in (8) and (16).

The second NLBC method can be used to accommodate a rough interface along  $z = z_b$  [12]. For a pressure-release boundary, the reflection coefficient can be modeled by [1, p. 54]

$$(17) \quad R_r(s) = -\exp\left[-\frac{1}{2}\Gamma^2(s)\right],$$

where  $\Gamma(s) = 2\sigma\gamma_-(s)$  is the Rayleigh parameter and  $\sigma$  is the rms roughness of the boundary. The impedance corresponding to (17) becomes

$$(18) \quad G_r(s) = \frac{1}{i\gamma_-(s)} \tanh\left[\frac{1}{4}\Gamma^2(s)\right].$$

Finally, we consider the region  $z > z_b$  to be occupied by an inhomogeneous medium described by the profile  $N^2(z) - 1 = \beta + \mu(z - z_b)$  [13, 14]. In this case, the reflection coefficient involves the Airy function  $\text{Ai}$  and can be written in the form

$$(19) \quad R_i(s) = \frac{i\gamma_-(s) - (\rho_-/\rho_+)sW(s)}{i\gamma_-(s) + (\rho_-/\rho_+)sW(s)},$$

where  $W(s) \equiv \{\partial_z \text{Ai}[\zeta(s)]\} / \{s \text{Ai}[\zeta(s)]\}$ ,  $\zeta(s) = \beta/\mu + 2ik_0s/\tau$ ,  $\tau = (\mu k_0^2)^{1/3} e^{-\pi i/3}$  for  $\mu > 0$  and  $\tau = (-\mu k_0^2)^{1/3}$  when  $\mu < 0$ . The  $G_i(s)$  that corresponds to (19) leads to the non-local boundary condition in the form [13]

$$(20) \quad \partial_z \psi(r, z_b) = \int_0^r \partial_r \psi(r, z_b) w(t - r, z_b) dt.$$

The kernel is given by  $w(r, z_b) = \tau \{ \text{Ai}'(\xi) / \text{Ai}(\xi) + \sum_m^\infty \exp[(x_m - \xi)r\tau^2/2ik_0] / (x_m - \xi) \}$  where  $\xi = \beta\tau/\mu$  and  $x_m$  are the zeros of the Airy function.

## 4 Example

To demonstrate the use of an NLBC for an inhomogeneous medium, we consider sound propagating in a surface duct overlying an upward-refracting linear- $N^2$  half-space. Within the duct, the sound speed profile is given by  $c(z) = 1536.5 + 0.018z$  m s<sup>-1</sup>. The constant gradient of  $N^2$  in the lower half-space is  $\mu = -0.0002$  m<sup>-1</sup>. The transmission losses ( $-10 \log_{10} |p|^2$ ) shown in Fig. 1 were generated at a frequency of 300 Hz and a source depth of 91.44 m. The results in the left panel were computed using a wavenumber integration code [1, pp. 203–270] and depict a portion of the upward-refracting region below  $z = z_b$ . The NLBC for the PE was evaluated along the bottom of the duct at  $z_b = 152.5$  m. The PE+NLBC predictions shown in the right panel clearly reveal that the NLBC correctly accounts for the energy that is refracted upwards from the lower medium without extending the computational grid into the region  $z > z_b$ .

## 5 Conclusions

We have described two methods for deriving non-local boundary conditions that reduce the computational domain for predicting one-way wave propagation in a leaky waveguide. Although the development was carried out for the standard PE, both methods can be applied to the rational-linear PE [4, 6, 11]. At the present time, however, it is not clear how to apportion the NLBC for the total field among multiple Padé terms needed for solving higher-order PEs. This issue also needs to be addressed in order to take advantage of the improved capability of the split-step Padé PE algorithm [15].

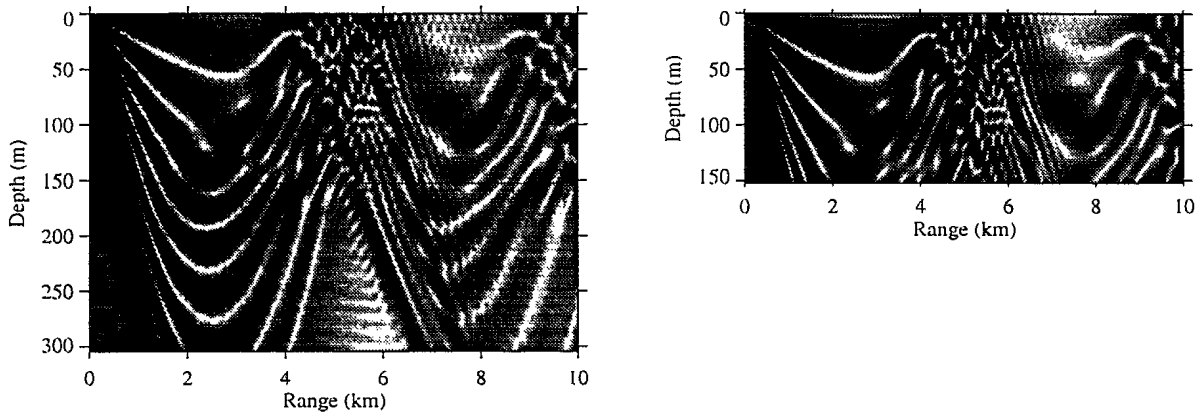


FIG. 1. SAFARI (left panel) vs PE+NLBC (right panel) transmission loss comparisons.

## References

- [1] F B. Jensen, W. A. Kuperman, M. B. Porter and H. Schmidt, *Computational Ocean Acoustics*, AIP Press, New York, 1994.
- [2] S. W. Marcus, *A generalized impedance method for application of the parabolic approximation to underwater acoustics*, J. Acoust. Soc. Am., 90 (1991), pp. 391–398.
- [3] V. A. Baskakov and A. V. Popov, *Implementation of transparent boundaries for numerical solution of the Schrodinger equation*, Wave Motion, 14 (1991), pp. 121–128.
- [4] J. S. Papadakis, *Exact, nonreflecting boundary conditions for parabolic-type approximations in underwater acoustics*, J. Comp. Acoust., 2 (1994), pp. 83–98.
- [5] M. D. Collins, *Benchmark calculations for higher-order parabolic equations*, J. Acoust. Soc. Am., 87 (1990), pp. 1535–1538.
- [6] D. Yeveck and D. J. Thomson, *Non-local boundary conditions for finite-difference PE solvers*, J. Acoust. Soc. Am., 101 (1997), p. 3182.
- [7] D. J. Thomson and M. E. Mayfield, *An exact radiation condition for use with the a posteriori PE method*, J. Comp. Acoust., 2 (1994), pp. 113–132.
- [8] J. S. Papadakis, M. I. Taroudakis, P. J. Papadakis and B. Mayfield, *A new method for a realistic treatment of the sea bottom in the parabolic approximation*, J. Acoust. Soc. Am., 92 (1992), pp. 2030–2038.
- [9] M. E. Mayfield and D. J. Thomson, *An FFT-based non-local boundary condition for the parabolic equation*, in 3rd European Conference on Underwater Acoustics, FORTH-IACM, Heraklion, 1996, pp. 237–242.
- [10] D. D. Ellis and D. M. F. Chapman, *A simple shallow water propagation model including shear wave effects*, J. Acoust. Soc. Am., 78 (1985), pp. 2087–2095.
- [11] A. Arnold and M. Ehrhardt, *Discrete transparent boundary conditions for wide angle “parabolic” equations in underwater acoustics*, preprint (1996).
- [12] M. F. Levy, *Modelling of rough surface effects with the matched transform PE*, in AGARD SPP Symposium on “Remote Sensing, a Valuable Source of Information,” Toulouse, France, 1996.
- [13] T. W. Dawson, D. J. Thomson and G. H. Brooke, *Non-local boundary conditions for acoustic PE predictions involving inhomogeneous layers*, in 3rd European Conference on Underwater Acoustics, FORTH-IACM, Heraklion, 1996, pp. 183–188.
- [14] M. F. Levy, *Transparent boundary conditions for parabolic equation solutions of radiowave propagation problems*, IEEE Trans. Antenn. Propag., 45 (1997), pp. 66–72.
- [15] M. D. Collins, *The split-step Padé solution for the parabolic equation method*, J. Acoust. Soc. Am., 93 (1993), pp. 1736–1742.

#587460